

Antiferromagnetism in $\text{Sr}_2\text{CuO}_2\text{Cl}_2$

D. Vaknin* and S. K. Sinha†

Exxon Research and Engineering Company, Annandale, New Jersey 08801

C. Stassis, L. L. Miller, and D. C. Johnston

Ames Laboratory and Department of Physics, Iowa State University, Ames, Iowa 50011

(Received 31 August 1989)

Magnetic-susceptibility $\chi(T)$ and neutron-diffraction studies on single-crystal specimens of $\text{Sr}_2\text{CuO}_2\text{Cl}_2$ are reported. A three-dimensional antiferromagnetic structure similar to that in La_2CuO_4 is identified below the Néel temperature $T_N = 251 \pm 5$ K by neutron diffraction, with an ordered moment $\mu(10 \text{ K}) = 0.34 \pm 0.04 \mu_B/\text{Cu}$ aligned along the [110] crystal direction. This moment is comparable to those for La_2CuO_4 samples with similar T_N . No structural transition from the tetragonal $I4/mmm$ space group is observed between 10 and 300 K. The $\chi(T)$ near T_N is consistent with the tetragonal structure, showing no evidence for the peak at T_N seen in orthorhombic La_2CuO_4 , arising from the Dzyaloshinsky-Moriya interaction, which is absent without the orthorhombic distortion. Above T_N the exchange coupling constant J between adjacent Cu ions is evaluated from $\chi(T)$ and found to be essentially identical to that in La_2CuO_4 . The anisotropic Cu spin and Van Vleck susceptibilities are also estimated from the analysis.

I. INTRODUCTION

Antiferromagnetic long-range order associated with the ordering of Cu^{2+} ions is by now known to be a property common to a variety of insulating members of the cuprate family of superconductors.¹⁻⁶ It has been demonstrated that above the Néel temperature T_N , the temperature-dependent magnetic susceptibilities $\chi(T)$ of these parent compounds are very similar to each other and are dominated by strong superexchange interactions between the Cu^{2+} spins in the CuO_2 planes.^{3,7-10} Inelastic neutron scattering¹¹⁻¹⁵ and other^{9,16,17} experiments indicate that the Cu ions comprise an antiferromagnetic two-dimensional (2D) spin- $\frac{1}{2}$ Heisenberg system on a

square lattice; the intraplanar Cu-Cu superexchange coupling constant J is many orders of magnitude larger than the anisotropy in J and the effective interplanar Cu-Cu coupling J_\perp . If the 3D antiferromagnetic order is driven by a very weak interplane superexchange coupling J_\perp , 3D order is expected to occur below a temperature T_N at which the intraplanar correlation length ξ is sufficiently large that $k_B T_N \sim J_\perp (\xi/d)^2$, where d is the Cu-Cu nearest-neighbor distance in the CuO_2 plane ($J_\perp \ll k_B T_N$).¹⁷ The small deviations from an ideal isotropic continuous 2D spin system should vary for the different cuprate structures, depending on the point symmetry of the Cu ions and the separation between adjacent magnetic layers. These can have significant effects on the

TABLE I. Comparison of some properties of La_2CuO_4 and $\text{Sr}_2\text{CuO}_2\text{Cl}_2$. a_{NN} and a_{NNN} are, respectively, the nearest-neighbor and next-nearest-neighbor Cu-Cu distances in the CuO_2 plane, and c_{NN} is the nearest-neighbor Cu-Cu distance between planes. T_N is the Néel temperature and μ is the ordered moment Cu at 10 K.

Space group	La_2CuO_4 <i>Cmca</i>	$\text{Sr}_2\text{CuO}_2\text{Cl}_2$ <i>I4/mmm</i>
Lattice parameters at 300 K (Å)	$a/\sqrt{2} = 3.7872$ $c/\sqrt{2} = 3.8192$ $b = 13.157$	$a = 3.975$ $c = 15.618$
a_{NN} (Å)	3.803	3.975
a_{NNN} (Å)	5.356 (5.401)	5.622
c_{NN} (Å)	7.103 (7.111)	8.30
T_N (K)	≈ 300	251-310
μ (μ_B)	≈ 0.6	0.34 (for $T_N = 251$ K)

physical properties. For instance, the orthorhombic distortion in La_2CuO_4 , which is associated with a rotation of the CuO_6 octahedra, gives rise to a Dzyaloshinsky-Moriya type of interaction, introducing antisymmetric as

well as anisotropic terms to the exchange interaction between spins in the plane.^{17,18} These interactions give rise to a small canting of the spins out of the CuO_2 plane below T_N in La_2CuO_4 , so that each plane exhibits a weak ferromagnetic component. These interactions also lead to the pronounced peak observed in $\chi(T)$ at T_N in this compound.

X-ray- and neutron-diffraction^{19,20} studies between 25 and 300 K have demonstrated that insulating²⁰ $\text{Sr}_2\text{CuO}_2\text{Cl}_2$ is a layered perovskite with the tetragonal ($I4/mmm$) $K_2\text{NiF}_4$ structure and is isostructural to the high-temperature form of La_2CuO_4 . As shown in Fig. 1(a), the structure contains CuO_2 planes with Cu in square-planar coordination with oxygen, a structural feature common to all high- T_c cuprates, but in $\text{Sr}_2\text{CuO}_2\text{Cl}_2$ these layers are separated by puckered SrCl rocksalt layers. The replacement of LaO in La_2CuO_4 by SrCl has a dramatic influence on the separation of the CuO_2 layers, as shown in Table I: The c -axis parameter is 18% larger than in La_2CuO_4 . There is also a significant increase by about 4% in the Cu-Cu nearest-neighbor distance compared to those in the superconducting cuprate systems. As our work and that of Ref. 20 shows, $\text{Sr}_2\text{CuO}_2\text{Cl}_2$ retains its tetragonal structure down to at least 10 K, in contrast to La_2CuO_4 , which transforms to the orthorhombic structure below 530 K.^{8,21} Exploring the similarities and differences between the magnetic properties of $\text{Sr}_2\text{CuO}_2\text{Cl}_2$ and those of the other cuprates like La_2CuO_4 should help to further our understanding of the electronic interactions in these important two-dimensional spin- $\frac{1}{2}$ systems. For example, the tetragonal structure of $\text{Sr}_2\text{CuO}_2\text{Cl}_2$ precludes the existence of the above-mentioned Dzyaloshinsky-Moriya interaction in this compound,¹⁷ and a comparison of its magnetic properties with those of La_2CuO_4 is therefore enlightening.

Herein, we present the results of a study of the magnetic properties of $\text{Sr}_2\text{CuO}_2\text{Cl}_2$ by neutron-diffraction and magnetization measurements. These experiments were performed on single-crystal specimens and powder samples prepared in Ames Laboratory as described elsewhere.²⁰

II. EXPERIMENTAL DETAILS

The magnetic susceptibility χ of three stacked crystals of total mass 40.73 mg was measured between 5 and 400 K in an applied magnetic field H of 5 kG using a Quantum Design SQUID magnetometer. Magnetization $M(H)$ isotherms were obtained between 5 and 400 K for $H \leq 50$ kG. The ferromagnetic impurity contribution to M was determined from the $M(H)$ isotherms and was found to be small, equivalent to that of 1 (6) at. ppm of Fe metal impurities with respect to Cu for $\mathbf{H} \parallel c$ ($\mathbf{H} \perp c$); these contributions are corrected for in Fig. 4, but not in Fig. 5.

The neutron-diffraction experiments were performed using the $H4S$ triple-axis spectrometer at the High Flux Beam Reactor at Brookhaven National Laboratory. Pyrolytic graphite was used as both monochromator and analyzer [(002) reflection]. The neutron wavelength, λ , was 2.37 Å. The $\lambda/2$ contamination of the incident beam

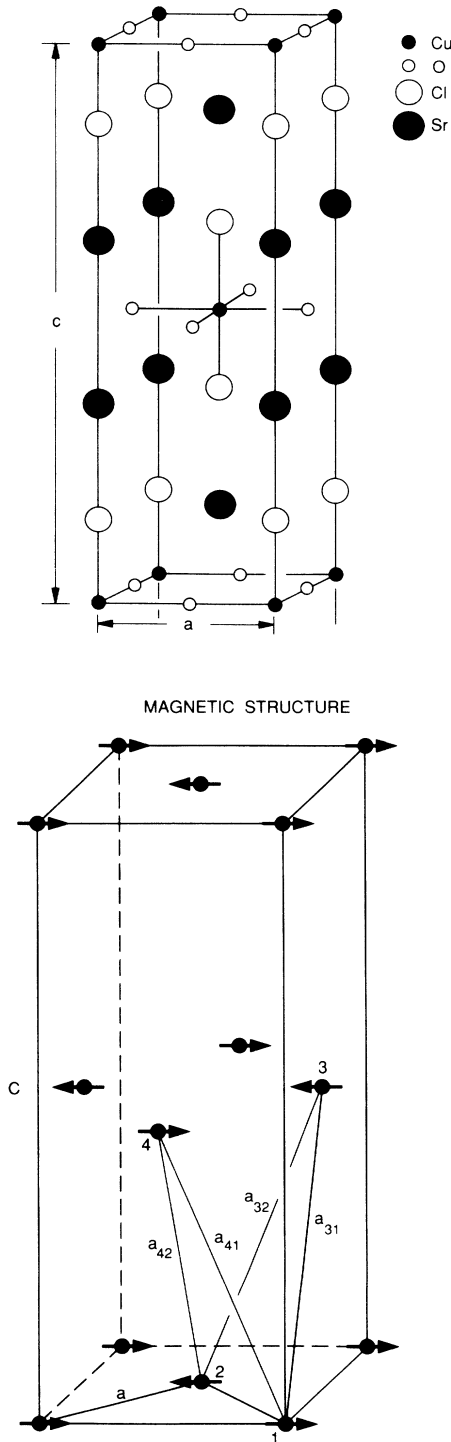


FIG. 1. Crystallographic (a) and magnetic (b) structures of $\text{Sr}_2\text{CuO}_2\text{Cl}_2$.

was practically eliminated by pyrolytic graphite filters. A single crystal of $\text{Sr}_2\text{CuO}_2\text{Cl}_2$ of mass 32 mg, with approximate dimensions $0.5 \times 0.5 \times 0.03 \text{ cm}^3$, was sealed in a container under helium atmosphere and mounted on a Displex closed-cycle refrigerator installed on the sample table of the spectrometer. From standard neutron-diffraction experiments at room temperature on this crystal as well as on a powder sample, we verified the structure of $\text{Sr}_2\text{CuO}_2\text{Cl}_2$ [Fig. 1(a)] determined by Grande and Müller-Buschbaum,¹⁹ with lattice parameters listed in Table I. No evidence was found between 10 and 300 K for the orthorhombic transition observed in La_2CuO_4 ; from our data, the upper limit for a possible distortion $|1 - a/b|$ is 0.002.

III. RESULTS AND DISCUSSION

A. Neutron-diffraction measurements

At low temperatures, the neutron-diffraction scans revealed a set of peaks not present in the room-temperature scans. These low-temperature diffraction peaks can be identified as $(\frac{1}{2} + h, \frac{1}{2} + k, l)$ reflections. On the other hand, we did not observe any $(\frac{1}{2} + h, \frac{1}{2} + k, \frac{1}{2} + l)$ reflections. These observations suggest that $\text{Sr}_2\text{CuO}_2\text{Cl}_2$ undergoes a transition to an antiferromagnetic state similar to that of the layered perovskites K_2NiF_4 , La_2CuO_4 , and La_2NiO_4 . The intensities of the magnetic peaks are consistent with a collinear spin structure with the ordered moment aligned in the [110] crystal direction and perpendicular to the antiferromagnetic propagation vector, as shown in Fig. 1(b). This magnetic structure is the same as that observed in La_2CuO_4 ,¹ except that in $\text{Sr}_2\text{CuO}_2\text{Cl}_2$ the absence of any orthorhombic distortion allows for the formation of two equivalent domains (accounted for in the calculation of the ordered moment), and precludes the development of a weak ferromagnetic moment in each CuO_2 layer as already noted.

The fact that $\text{Sr}_2\text{CuO}_2\text{Cl}_2$ remains tetragonal at and below T_N raises the question of how the correlated antiferromagnetic planes couple to give the unique 3D long-range order. Assuming that the intraplane magnetic structure (including the direction of the ordered moment) is determined solely by the intraplane interactions, there are two collinear configurations, *A* and *B*, for the stacking of the magnetic sheets (Fig. 2). In orthorhombic La_2CuO_4 , it is currently believed that exchange interactions are responsible for the coupling between planes. However, in the tetragonal phase, these sum to zero. We show here that a possible mechanism for the observed stacking configuration in the absence of orthorhombic distortion is the magnetic dipole-dipole interaction, which distinguishes between the two configurations in Fig. 2. Consider a moment μ in a layer aligned along the magnetic *a* axis. The energy of this moment in the presence of the dipolar field of the aligned out-of-plane Cu moments is

$$E_\alpha = -\mu \cdot \mathbf{B}_\alpha^{\text{loc}} = -\sum_i \mu \cdot \mu_{i\alpha} (3 \cos^2 \phi_i - 1) / r_i^3,$$

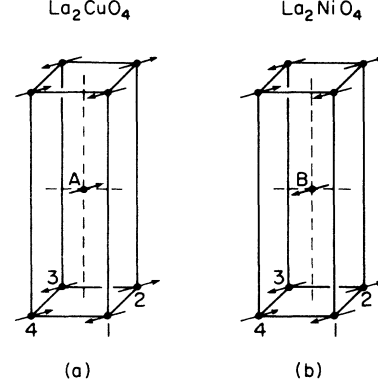


FIG. 2. Comparison of the magnetic structures of La_2CuO_4 (a) and La_2NiO_4 (b).

where the sum is over the Cu moments $\mu_{i\alpha}$ in other layers, $\alpha = A$ or B , r_i is the distance from the moment μ to the moment $\mu_{i\alpha}$, and ϕ_i is the angle between \mathbf{r}_i and the *a* axis. The sum was evaluated over an approximate radius of 70 Å for the two configurations *A* and *B*, leading to

$$E_A/k_B = -E_B/k_B = -\mu^2(0.19 \text{ mK}/\mu_B^2),$$

where the ordered moment μ is in units of μ_B . Thus, the magnetic structure of La_2CuO_4 in Fig. 2(a) is favored by the magnetic dipole interaction between layers over the magnetic structure of La_2NiO_4 in Fig. 2(b). If interlayer dipole coupling is solely responsible for the 3D interlayer ordering, one would expect that $k_B T_N \sim \pi |E_A| (\xi/d)^2$, or $\xi(T_N) \sim 3000 \text{ Å}$ in $\text{Sr}_2\text{CuO}_2\text{Cl}_2$, where, as mentioned above, ξ is the in-plane correlation length and d is the in-plane Cu-Cu distance. This $\xi(T_N)$ is of the right order of magnitude since $\xi(T_N \approx 200 \text{ K}) \sim 1000 \text{ Å}$ in La_2CuO_4 .¹² Furthermore, despite the large increase in the CuO_2 interplane distance in $\text{Sr}_2\text{CuO}_2\text{Cl}_2$ over that in La_2CuO_4 , the T_N values are comparable (Table I). This suggests that the interplane coupling leading to the three-dimensional ordering of the system is of long range. The interplanar magnetic dipole interaction therefore appears to be a viable candidate for inducing 3D order in both compounds. In this context, we remark that dipolar anisotropy within a single CuO_2 plane favors alignment parallel to the *c* axis rather than in the observed [110] alignment direction. The local field at a Cu site due to the ordered Cu moments in the same CuO_2 plane is calculated, as above, to be

$$B^{\text{loc}} = (195 \text{ G}/\mu_B) \mu (3 \cos^2 \theta - 1),$$

where θ is the angle between μ and the *c* axis. The corresponding effective anisotropy field is $H_A = (585 \text{ G}/\mu_B) \mu$ and energy $E/k_B = -\mu H_A/k_B = (-39 \text{ mK}/\mu_B^2) \mu^2$, which are a factor of 100 larger than calculated above for the interlayer dipole interaction. This preference for moment alignment along the *c* axis is evidently counteracted by other sources of intralayer alignment anisotropy.

The values of μf , the product of the ordered moment μ and the magnetic form factor f , determined from the integrated intensities of the magnetic reflections measured

TABLE II. The product of the ordered magnetic moment μ at 10 K and the form factor f determined from the magnetic neutron reflections assuming the magnetic structure of Fig. 1(b). The form factors f^* and f^+ are those of Cu^{2+} in K_2CuF_4 [J. Akimitsu and Y. Ito, J. Phys. Soc. Jpn. **40**, 1621 (1976)] and in $\text{Sr}_2\text{CuO}_2\text{Cl}_2$, respectively.

(h, k, l)	$\sin(\theta)/\lambda$	(μf)	f^*	f^+
$(\frac{1}{2}, \frac{1}{2}, 0)$	0.089	0.28(1)	0.83	0.83(6)
$(\frac{1}{2}, \frac{1}{2}, 1)$	0.095	0.25(2)	0.82	0.74(7)
$(\frac{1}{2}, \frac{1}{2}, 2)$	0.110	0.23(2)	0.80	0.68(5)
$(\frac{1}{2}, \frac{1}{2}, 3)$	0.132	0.23(4)	0.77	0.68(10)
$(\frac{1}{2}, \frac{1}{2}, 4)$	0.156	0.25(4)	0.74	0.68(11)
$(\frac{1}{2}, \frac{1}{2}, 5)$	0.184	0.20(3)	0.70	0.59(9)
$(\frac{3}{2}, \frac{3}{2}, 0)$	0.269	0.11(2)	0.57	0.32(10)
$(\frac{3}{2}, \frac{3}{2}, 1)$	0.270	a	0.57	a
$(\frac{3}{2}, \frac{3}{2}, 2)$	0.274	0.14(2)	0.55	0.41(8)

^aThe scattering vector $(\frac{3}{2}, \frac{3}{2}, 1)$ is almost parallel to the spin direction \mathbf{S} , making it impossible to observe any peak, in support of our model for the magnetic structure.

at 10 K, are listed in Table II. Assuming a Cu^{2+} magnetic form factor, the magnetic moment was found to be $0.34 \pm 0.04 \mu_B/\text{Cu}$, a value consistent with that estimated from the $(\frac{1}{2}, \frac{1}{2}, 0)$ reflection of a 30 g powder sample. As in the case of La_2CuO_4 , the fit of the experimental data by the Cu^{2+} magnetic form factor is not satisfactory (see Table II). The relatively limited range of $(\sin\theta)/\lambda$ values (0.1–0.27) covered by the reflections studied in the present experiment, however, does not allow us to draw more definitive conclusions regarding the magnetic form factor. A more detailed study of the magnetic form factor was performed at the Intense Pulsed Neutron Source of Argonne National Laboratory.²²

The variation of the $(\frac{1}{2}, \frac{1}{2}, 0)$ magnetic peak intensity with temperature is shown in Fig. 3. The data are quite well fitted (Fig. 3, solid curve) by a function of the form $A(1 - T/T_N)^{2\beta}$, with $T_N = 251 \pm 5$ K and $\beta = 0.30 \pm 0.02$.

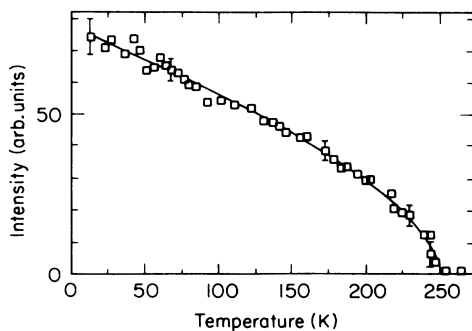


FIG. 3. Temperature dependence of the integrated intensity of the $(\frac{1}{2}, \frac{1}{2}, 0)$ magnetic neutron-diffraction peak for a single-crystal specimen of $\text{Sr}_2\text{CuO}_2\text{Cl}_2$. The solid curve is a fit of the quantity $A(1 - T/T_N)^{2\beta}$ to the data, where $T_N = 251$ K and $\beta = 0.30$.

Above T_N and up to 300 K, some intensity, decreasing with increasing temperature, is observed at the $(\frac{1}{2}, \frac{1}{2}, 0)$ position. There is no tendency of the order parameter to saturate at low temperatures.

B. Magnetic susceptibility measurements

The magnetic susceptibility $\chi(T)$ for $\text{Sr}_2\text{CuO}_2\text{Cl}_2$ for $\mathbf{H} \parallel \mathbf{c}$ and $\mathbf{H} \perp \mathbf{c}$ are shown in Fig. 4(a). The data increase linearly from ≈ 310 K to at least 400 K. The positive curvature below ≈ 200 K is attributed primarily to the Curie-Weiss contribution $[C/(T - \Theta)]$ from nearly isolated Cu^{2+} (spin $\frac{1}{2}$) defects and/or Cu in impurity phase inclusions from the flux growth. The Curie constants C were found to be $6.95 \times 10^{-4} \text{ cm}^3 \text{ K/mol}$ ($1.24 \times 10^{-3} \text{ cm}^3 \text{ K/mol}$) for $\mathbf{H} \parallel \mathbf{c}$ ($\mathbf{H} \perp \mathbf{c}$), with Weiss temperatures $\Theta = 0$ K (-4.6 K). The data corrected for these impurity terms χ^{corr} are plotted in Fig. 4(b), where the data for $\mathbf{H} \parallel \mathbf{c}$ ($\mathbf{H} \perp \mathbf{c}$) are denoted by χ_c (χ_{ab}). A distinct slope discontinuity is seen in χ_c at the Néel temperature $T_N \approx 310$ K, a somewhat higher T_N than found (251 K) for the (different) 32 mg crystal measured in this neutron-diffraction study. This apparent variability in

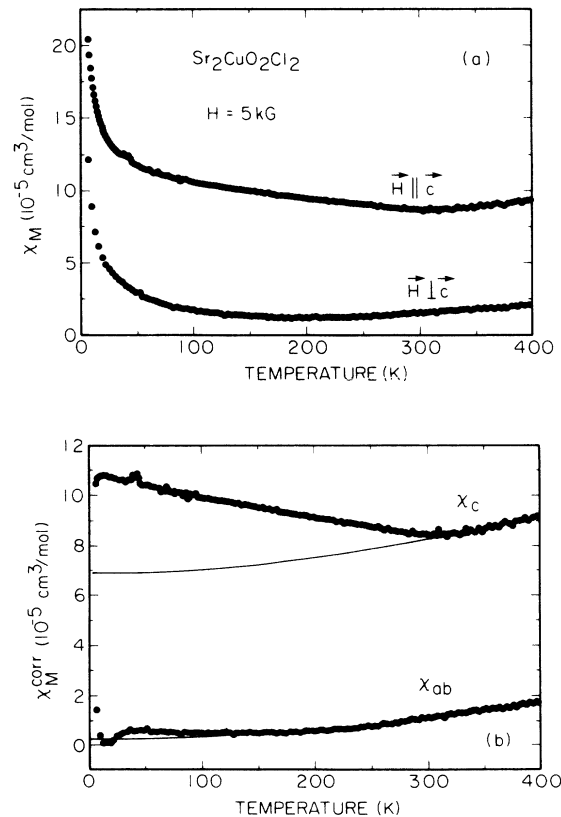


FIG. 4. Measured χ_M (a) and corrected χ_M^{corr} (b) molar magnetic susceptibility vs temperature for $\text{Sr}_2\text{CuO}_2\text{Cl}_2$. The solid curves are theoretical fits to the data above 320 K; below $T_N \approx 310$ K, the curves represent the behavior expected in the absence of static antiferromagnetic ordering.

T_N is presumably associated with minor differences in composition; in La_2CuO_4 , T_N can vary from ≈ 0 to 300 K with very small changes (1%) in composition.^{7,8} Above 320 K, the slopes $d\chi/dT$ in Fig. 4(b) are significantly different for the two field directions: $d\chi_c/dT = (9.0 \pm 0.5) \times 10^{-8} \text{ cm}^3/\text{mole K}$ and $d\chi_{ab}/dT = (6.0 \pm 0.03) \times 10^{-8} \text{ cm}^3/\text{mol K}$. This difference suggests the presence of anisotropy in the Cu^{2+} spectroscopic splitting factor g (see the following). The average anisotropy

$$\Delta\chi \equiv \chi_c - \chi_{ab}$$

between 320 and 400 K is $7.2 \times 10^{-5} \text{ cm}^3/\text{mol}$. $\Delta\chi$ increases with decreasing T below T_N , and therefore behaves qualitatively as expected if the ordered moment is aligned within the a - b plane, in agreement with the ordering direction inferred from our neutron-diffraction measurements. The origin of $\Delta\chi$ above T_N is most probably anisotropy in the temperature-independent Van Vleck paramagnetism of the Cu^{2+} ions and anisotropy in the spin susceptibility arising from an anisotropic g factor of these ions, as discussed in more detail in the following. Neither χ_c nor χ_{ab} show any discernible peak at or near T_N , in contrast to the large peaks seen at T_N for La_2CuO_4 . Since we did not detect any orthorhombic distortion in $\text{Sr}_2\text{CuO}_2\text{Cl}_2$, this observation supports the notion that the peak seen in La_2CuO_4 is due to the Dzyaloshinsky-Moriya type of interaction, which is absent without the orthorhombic distortion.^{17,18}

$M(H)$ data for $\text{H} \perp c$, shown in Fig. 5, exhibit a change in slope below $\approx 7 \text{ kG}$ for data below $\sim 100 \text{ K}$; for $\text{H} \parallel c$, the $M(H)$ data do not exhibit these slope discontinuities. Thus, the probable origin of the slope discontinuities for $\text{H} \perp c$ (i.e., for \mathbf{H} in the plane of the ordered moment below T_N) is a spin-flop transition where the spin components that are initially parallel to the applied magnetic field begin to change to an orientation perpendicular to the field; further measurements are in progress to test this hypothesis.

To analyze the $\chi(T)$ data, we assume that χ in the a - or c -axis directions is the sum of three contributions

$$\chi(T) = \chi^{\text{dia}} + \chi^{\text{VV}} + \chi^{\text{spin}}(T), \quad (1)$$

where χ^{dia} is the isotropic diamagnetic core contribution, χ^{VV} is the anisotropic Van Vleck paramagnetism of the Cu^{2+} ions, and $\chi^{\text{spin}}(T)$ is the temperature-dependent, and in general anisotropic, spin susceptibility of the Cu^{2+} $S = \frac{1}{2}$ spin sublattice. Both χ^{dia} and χ^{VV} are assumed to be independent of temperature. In La_2CuO_4 , neutron scattering and other measurements have shown that the anisotropy in the Cu-Cu exchange interaction constant J is very small, as already noted. Since J is determined primarily by electronic interactions within the CuO_2 layers,³ J is expected to be nearly isotropic in $\text{Sr}_2\text{CuO}_2\text{Cl}_2$ as well. Thus, above T_N we take $\chi^{\text{spin}}(T)$ to be the spin susceptibility $\chi^{2D}(T)$ of the spin- $\frac{1}{2}$ Heisenberg square lattice antiferromagnet for which the interaction between nearest-neighbor spins is written here as $2JS_i \cdot S_j$.

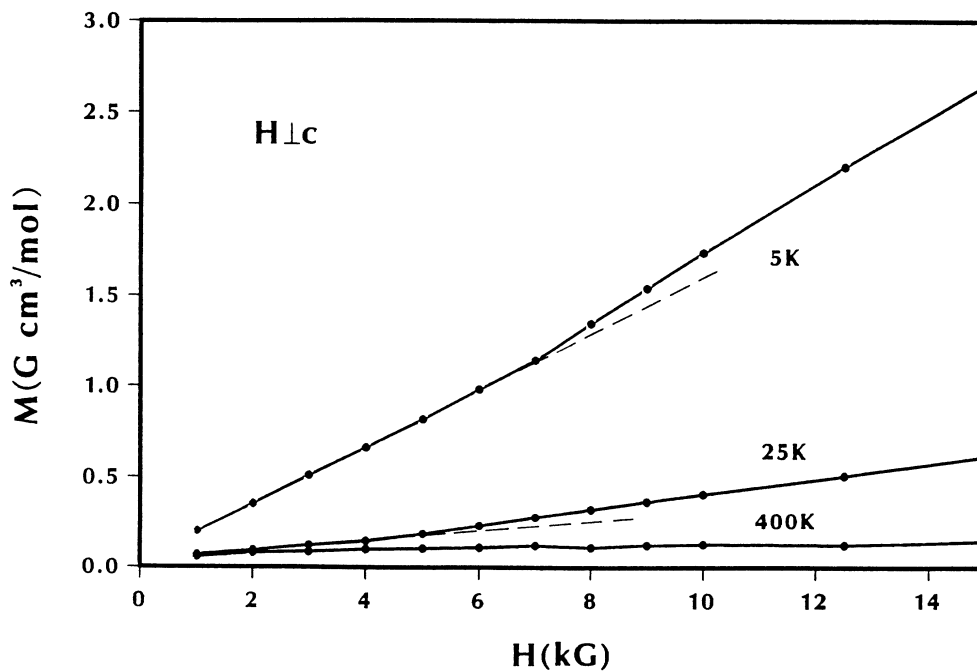


FIG. 5. Molar magnetization isotherms for $\text{Sr}_2\text{CuO}_2\text{Cl}_2$ with $\text{H} \perp c$ axis, showing slope changes near 7 and 4 kG at temperatures of 5 and 25 K, respectively. The dashed lines highlight the field-induced transitions.

$\chi^{2D}(T)$ has the form^{9,23}

$$\chi_{\alpha}^{2D}(T) = 0.0469(N_A g_{\alpha}^2 \mu_B^2 / J k_B) F(T/T^{\max}), \quad (2)$$

where here $\alpha = c$ or ab , $F(z)$ is a function with a maximum value of 1 at the temperature T^{\max} at which χ^{2D} reaches its maximum value χ_{\max}^{2D} , J is in degrees Kelvin, $T^{\max} = 1.86$ J, and χ_{\max}^{2D} is the prefactor to $F(z)$ in Eq. (2).

From Eq. (2), anisotropy in $\chi^{\text{spin}}(T)$ above T_N can occur if $g_c \neq g_{ab}$, where g_c (g_{ab}) is the g factor of the Cu²⁺ ion with $\mathbf{H} \parallel \mathbf{c}$ ($\mathbf{H} \perp \mathbf{c}$). Thus, the large anisotropy in Fig. 4(b) above T_N can arise from χ^{spin} as well as χ^{VV} . To estimate the magnitudes of the various parameters, we first assume g to be isotropic ($g_c = g_{ab} = 2$). Fitting Eq. (1) [with $\chi^{\text{spin}}(T)$ given by $\chi^{2D}(T)$ in Eq. (2) from Ref. 9] to the χ_c and χ_{ab} data above 320 K leads to the ($\chi^{\text{VV}} + \chi^{\text{dia}}$) values for the two directions and J value in Table III; for this case the χ anisotropy ($\Delta\chi^{\text{VV}}$) above T_N arises solely from χ^{VV} .

In the ordered state below T_N , the ordered moment is in the [110] direction; hence, one must distinguish this direction from the uniaxial crystal c axis. The value of $\chi_{\perp}(0)$, the spin susceptibility in the 3D antiferromagnetically ordered state with \mathbf{H} perpendicular to the ordering direction at $T=0$, may be calculated from the fit to the data above T_N using²³

$$\chi_{\perp,\alpha}(0) \simeq \chi_{\perp,\alpha}^0 (1 - \Delta S/S),$$

where $\alpha = ab$ or c ,

$$\chi_{\perp,\alpha}^0 = N_A g_{\alpha}^2 \mu_B^2 / 16 k_B J = (0.0234 \text{ cm}^3 \text{ K/mol}) g_{\alpha}^2 / J \quad (3)$$

is the mean-field value, and $\Delta S/S \simeq 0.4$ (Ref. 24) is the zero-point spin deviation. Using $g_c = g_{ab} = 2$ and $J = 860$ K yields $\chi_{\perp,c}(0) = \chi_{\perp,ab}(0) = 6.5 \times 10^{-5} \text{ cm}^3/\text{mol}$. Because the ordered moment is aligned in the a - b plane,

$$\begin{aligned} \chi_c(0) &= \chi^{\text{dia}} + \chi_c^{\text{VV}} + \chi_{\perp,c}(0), \\ \chi_{ab}(0) &= \chi^{\text{dia}} + \chi_{ab}^{\text{VV}} + \chi_{\perp,ab}(0)/2, \end{aligned} \quad (4)$$

where $\chi_{\parallel}(0)$ is assumed to be zero¹⁴ and the term $\chi_{\perp,ab}(0)/2$ at the end of Eqs. (4) arises from the presence of antiferromagnetic domains with orthogonal alignment directions within the a - b plane. Thus,

$$\begin{aligned} \Delta\chi(0) &= \chi_c(0) - \chi_{ab}(0) \\ &= \Delta\chi^{\text{VV}} + \chi_{\perp,c}(0) - \chi_{\perp,ab}(0)/2. \end{aligned} \quad (5)$$

Using $\Delta\chi^{\text{VV}} = 7.3 \times 10^{-5} \text{ cm}^3/\text{mol}$ from Table III and the preceding calculated $\chi_{\perp}(0)$ predicts that $\Delta\chi(0) \simeq 10.5 \times 10^{-5} \text{ cm}^3/\text{mol}$, in good agreement with the observed value [Fig. 4(b)] of $(10 \pm 1) \times 10^{-5} \text{ cm}^3/\text{mol}$.

On the other hand, the existence of a large anisotropy in χ^{VV} suggests that significant anisotropy should also be present in the Cu²⁺ g factor, since spin-orbit coupling is strong for Cu²⁺. Anisotropy in g is also indicated by the anisotropy in $d\chi/dT$ in Fig. 4(b) above 320 K as already noted, and by the anisotropic g values ($g > 2$) found²⁵ in elongated octahedral complexes of Cu²⁺. Increasing g has the effect of increasing the J necessary to fit Eq. (1) to the data above T_N . An upper limit to J may be that in La₂CuO₄. A recent inelastic neutron scattering study of this compound yielded an accurate spin-wave velocity $d\omega/dk = (0.85 \pm 0.03) \text{ eV \AA}/\hbar$ ¹⁵. Using the dispersion relation $\omega = (2^{3/2} J a k)$ and $a = 3.8 \text{ \AA}$ appropriate to the Cu²⁺ spin- $\frac{1}{2}$ square lattice in La₂CuO₄ leads to $J = 79 \text{ meV}$ (920 K), slightly larger than the value in Table III derived above for Sr₂CuO₂Cl₂. Setting $J = 920$ K and fitting Eq. (1), as above, to the data in Fig. 4(b) between 320 and 400 K yield the g_c , g_{ab} , and ($\chi^{\text{dia}} + \chi^{\text{VV}}$) values in Table III, where $\langle g \rangle = 2.16$, similar to $\langle g \rangle$ in elongated distorted octahedral complexes of Cu²⁺.²⁵ The g values may be compared with $g_c = 2.29$ and $g_{ab} = 2.03$ found at 100 K for isolated Cu²⁺ defects in a single crystal of YBa₂Cu₃O_{6.35}.²⁶ The fits are shown as the solid curves in Fig. 4(b); below T_N , the curves represent the behavior expected in the absence of static antiferromagnetic order. Using g_c and g_{ab} from Table III and $J = 920$ K in Eqs. (3) yields $\chi_{\perp,c}(0) = 9.2 \times 10^{-5} \text{ cm}^3/\text{mol}$ and $\chi_{\perp,ab}(0) = 6.2 \times 10^{-5} \text{ cm}^3/\text{mol}$. Equation (5) and $\Delta\chi^{\text{VV}} = 5.0 \times 10^{-5} \text{ cm}^3/\text{mol}$ from Table III then predict $\Delta\chi(0) = 11.1 \times 10^{-5} \text{ cm}^3/\text{mol}$, again in good agreement with the observed value in Fig. 4(b). Between 320 and 400 K, the anisotropy in g leads to anisotropy in the spin susceptibility $\Delta\chi^{\text{spin}} = \Delta\chi - \Delta\chi^{\text{VV}} \simeq 2.2 \times 10^{-5} \text{ cm}^3/\text{mol}$, or about 30% of the total observed anisotropy. Up to now, anisotropy in g has been neglected in analyses of anisotropy in the susceptibility of the high- T_c cuprates;²⁷ however, our analysis suggests that it may be appreciable.

The values of χ^{VV} obtained from Table III assuming

TABLE III. Fitting parameters for the magnetic susceptibility data in Fig. 4(b) between 320 K and 400 K. The χ^{VV} values were computed from the second column of data assuming that $\chi^{\text{dia}} = -11.7 \times 10^{-5} \text{ cm}^3/\text{mol}$ using Ref. 28.

	g	$(\chi^{\text{VV}} + \chi^{\text{dia}})$ ($10^{-5} \text{ cm}^3/\text{mol}$)	J (K)	$\Delta\chi^{\text{calc}}(0)$ ($10^{-5} \text{ cm}^3/\text{mol}$)	χ^{VV} ($10^{-5} \text{ cm}^3/\text{mol}$)
$\mathbf{H} \parallel \mathbf{c}$	$\equiv 2$	3.7	860	10.5	15.4
$\mathbf{H} \perp \mathbf{c}$	$\equiv 2$	-3.6			
$\mathbf{H} \parallel \mathbf{c}$	2.46	1.9	$\equiv 920$	11.1	13.6
$\mathbf{H} \perp \mathbf{c}$	2.01	-3.1			

that $\chi^{\text{dia}} = -11.7 \times 10^{-5} \text{ cm}^3/\text{mol}$ (Ref. 28) are listed in Table III. For both sets of fitting parameters in Table III, the χ^{VV} and $\Delta\chi^{\text{VV}}$ values are much larger than values obtained from spin-polarized band calculations for Sr_2CuO_4 ,²⁹ which are $\chi_c^{\text{VV}} = 4.0 \times 10^{-5} \text{ cm}^3/\text{mol}$ and $\chi_{ab}^{\text{VV}} = 1.5 \times 10^{-5} \text{ cm}^3/\text{mol}$, yielding $\Delta\chi^{\text{VV}} = 2.5 \times 10^{-5} \text{ cm}^3/\text{mol}$. Furthermore, from crystal-field considerations, one expects the ratio $\chi_c^{\text{VV}}/\chi_{ab}^{\text{VV}} > 4$,^{25,27} in contrast to values < 2 in Table III. On the other hand, the $\Delta\chi^{\text{VV}}$ values are comparable with those estimated for the Cu(2) ions in the CuO_2 planes of $\text{YBa}_2\text{Cu}_3\text{O}_7$.²⁷ Thus, the value of $|\chi^{\text{dia}}|$ just used to compute the χ^{VV} values in Table III may be too large.

IV. CONCLUDING REMARKS

The preceding agreement between the observed value of $\Delta\chi(0) \equiv \chi_c(0) - \chi_{ab}(0)$ and those calculated from the fits to the data above T_N suggests that the magnetic system in $\text{Sr}_2\text{CuO}_2\text{Cl}_2$ is well described as being a spin- $\frac{1}{2}$ Heisenberg square lattice antiferromagnet, with a weak interplane coupling which results in 3D order. Theoretical calculations¹⁴ indicate that at $T=0$, the ordered moment should be that of an ordered 2D antiferromagnetic system; spin wave and other theory^{23,24} predicts that this moment should be $\approx 0.6 \mu_B/\text{Cu}$. That the ordered moment from our neutron-diffraction study is much smaller than this value indicates that there is a much more disorder than predicted by spin-wave theory. This may be re-

lated to interlayer magnetic frustration arising from the tetragonal crystal structure and/or defects. A similar effect has been documented in La_2CuO_4 (Ref. 30) and $\text{YBa}_2\text{Cu}_3\text{O}_{6+x}$;⁴ it is interesting that our value $\mu = 0.34 \mu_B$ for $T_N = 251 \text{ K}$ is similar to values for La_2CuO_4 and $\text{YBa}_2\text{Cu}_3\text{O}_{6+x}$ samples with similar T_N values.^{4,31} If, for example, there were stacking disorder of the antiferromagnetic sheets along the c axis, one would expect to see diffuse scattering along the $(\frac{1}{2}, \frac{1}{2}, l)$ rods, as observed in $\text{YBa}_2\text{Cu}_3\text{O}_{6+x}$.⁴ Alternatively, the microscopic moment of $0.34 \mu_B/\text{Cu}$ could be uniform throughout the volume of the crystal, where the reduction from the predicted spin wave value of $\approx 0.6 - 0.7 \mu_B/\text{Cu}$ could arise from an as yet unidentified mechanism; in this case, our analysis of $\Delta\chi(0)$ above would have to be modified accordingly. Neutron-scattering experiments on large single crystals of $\text{Sr}_2\text{CuO}_2\text{Cl}_2$ should be able to differentiate between these possibilities.

ACKNOWLEDGMENTS

Work at Brookhaven was supported by the Division of Materials Sciences, U.S. Department of Energy (DOE) under Contract No. DE-AC02-76CH00016. Ames Laboratory is operated for the U. S. Department of Energy by Iowa State University under Contract No. W-7405-Eng-82. Work at Ames was supported by the Director for Energy Research, Office of Basic Energy Sciences.

*Also at the Laboratory for Research on the Structure of Matter, University of Pennsylvania, Philadelphia, PA 19104.

†Also at Physics Department, Brookhaven National Laboratory, Upton, NY 11973.

¹D. Vaknin, S. K. Sinha, D. E. Moncton, D. C. Johnston, J. M. Newsam, C. R. Safinya, and H. E. King, Jr., *Phys. Rev. Lett.* **58**, 2802 (1987); S. Mitsuda, G. Shirane, S. K. Sinha, D. C. Johnston, M. S. Alvarez, D. Vaknin, and D. E. Moncton, *Phys. Rev. B* **36**, 822 (1987).

²J. M. Tranquada, D. E. Cox, W. Kunnmann, H. Moudden, G. Shirane, M. Suenaga, P. Zolliker, D. Vaknin, S. K. Sinha, M. S. Alvarez, A. J. Jacobson, and D. C. Johnston, *Phys. Rev. Lett.* **60**, 156 (1988); J. W. Lynn and W.-H. Li, *J. Appl. Phys.* **64**, 6065 (1988), and references cited.

³D. Vaknin, E. Caignol, P. K. Davies, J. E. Fischer, D. C. Johnston, and D. P. Goshorn, *Phys. Rev. B* **39**, 9122 (1989).

⁴J. Rossat-Mignod, P. Burllet, M. J. Jurgens, C. Vettier, L. P. Regnault, J. Y. Henry, C. Ayache, L. Forro, H. Noel, M. Potel, P. Gougeon, and J. C. Levet, *J. Phys. (Paris) Colloq. C 8*, Suppl. 12 **49**, C8-2119 (1988), and references cited.

⁵N. Nishida, H. Miyatake, D. Shimada, S. Okuma, M. Ishikawa, T. Takatake, Y. Nakazawa, Y. Kuno, R. Keitel, J. G. Brewer, T. R. Riseman, D. L. Williams, and Y. Watanabe, *J. Phys. Soc. Jpn.* **57**, 722 (1988).

⁶G. M. Luke, B. J. Sternlieb, Y. J. Uemura, J. H. Brewer, R. Kadono, R. F. Kiefl, S. R. Kretzman, T. M. Riseman, J. Gopalakrishnan, A. W. Sleight, M. A. Subramanian, S. Uchida, H. Takagi, and Y. Tokura, *Nature* **338**, 49 (1989); B. X. Yang, R. F. Kiefl, J. H. Brewer, J. F. Carolan, W. N. Hardy, R. Kadono, J. R. Kempton, S. R. Kretzman, G. M. Luke, T.

M. Riseman, D. L. Williams, Y. J. Uemura, B. Sternlieb, M. A. Subramanian, A. R. Strzelecki, J. Gopalakrishnan, and A. W. Sleight, *Phys. Rev. B* **39**, 847 (1989).

⁷D. C. Johnston, J. P. Stokes, D. P. Goshorn, and J. T. Lewandowski, *Phys. Rev. B* **36**, 4007 (1987).

⁸D. C. Johnston, S. K. Sinha, A. J. Jacobson, and J. M. Newsam, *Physica C* **153-155**, 572 (1988).

⁹D. C. Johnston, *Phys. Rev. Lett.* **62**, 957 (1989).

¹⁰J. M. Tranquada, A. H. Moudden, A. I. Goldman, P. Zolliker, D. E. Cox, G. Shirane, S. K. Sinha, D. Vaknin, D. C. Johnston, M. S. Alvarez, A. J. Jacobson, J. T. Lewandowski, and J. M. Newsam, *Phys. Rev. B* **38**, 2477 (1988).

¹¹G. Shirane, Y. Endoh, R. J. Birgeneau, M. A. Kastner, Y. Hidaka, M. Oda, M. Suzuki, and T. Murakami, *Phys. Rev. Lett.* **59**, 1613 (1987); M. Soto, S. Shamoto, J. M. Tranquada, G. Shirane, and B. Keimer, *ibid.* **61**, 1317 (1988).

¹²Y. Endoh, K. Yamada, R. J. Birgeneau, D. R. Gabbe, H. P. Jenssen, M. A. Kastner, C. J. Peters, P. J. Picone, T. R. Thurston, J. M. Tranquada, G. Shirane, Y. Hidaka, M. Oda, Y. Enomoto, M. Suzuki, and T. Murakami, *Phys. Rev. B* **37**, 7443 (1988); R. J. Birgeneau, D. R. Gabbe, H. P. Jenssen, M. A. Kastner, P. J. Picone, T. R. Thurston, G. Shirane, Y. Endoh, M. Sato, K. Yamada, Y. Hidaka, M. Oda, Y. Enomoto, M. Suzuki, and T. Murakami, *ibid.* **38**, 6614 (1988).

¹³C. J. Peters, R. J. Birgeneau, M. A. Kastner, H. Yoshizawa, Y. Endoh, J. Tranquada, G. Shirane, Y. Hidaka, M. Oda, M. Suzuki, and T. Murakami, *Phys. Rev. B* **37**, 9761 (1988).

¹⁴S. Chakravarty, B. I. Halperin, and D. R. Nelson, *Phys. Rev. Lett.* **60**, 1057 (1988); *Phys. Rev. B* **39**, 2344 (1989).

¹⁵G. Aeppli, S. M. Hayden, H. A. Mook, Z. Fisk, S.-W. Cheong,

- D. Rytz, J. P. Remeika, G. P. Espinosa, and A. S. Cooper, *Phys. Rev. Lett.* **62**, 2052 (1989).
- ¹⁶R. T. Collins, Z. Schlesinger, M. W. Shafer, and T. R. McGuire, *Phys. Rev. B* **37**, 5817 (1988); K. B. Lyons, P. E. Sulewski, P. A. Fleury, H. L. Carter, A. S. Cooper, G. P. Espinosa, Z. Fisk, and S.-W. Cheong, *ibid.* **39**, 9693 (1989), and references cited; R. R. P. Singh, P. A. Fleury, K. B. Lyons, and P. E. Sulewski, *Phys. Rev. Lett.* **62**, 2736 (1989).
- ¹⁷T. Thio, T. R. Thurston, N. W. Preyer, P. J. Picone, M. A. Kastner, H. P. Jenssen, D. R. Gabbe, C. Y. Chen, R. J. Birgeneau, and A. Aharony, *Phys. Rev. B* **38**, 905 (1988); S.-W. Cheong, J. D. Thompson, and Z. Fisk, *ibid.* **39**, 4395 (1989).
- ¹⁸M. A. Kastner, R. J. Birgeneau, T. R. Thurston, P. J. Picone, H. P. Jenssen, D. R. Gabbe, M. Sato, K. Fukuda, S. Shamoto, Y. Endoh, K. Yamada, and G. Shirane, *Phys. Rev. B* **38**, 6636 (1988).
- ¹⁹B. Grande and Hk. Müller-Buschbaum, *Z. Anorg. Allg. Chem.* **417**, 68 (1975).
- ²⁰L. L. Miller, X. L. Wang, S. X. Wang, C. Stassis, D. C. Johnston, J. Faber, Jr., and C.-K. Loong (submitted to *Phys. Rev. B*).
- ²¹J. M. Longo and P. M. Raccach, *J. Solid State Chem.* **6**, 526 (1973).
- ²²X. L. Wang, L. L. Miller, C. Stassis, D. C. Johnston, A. J. Schultz, and C.-K. Loong (unpublished).
- ²³L. J. de Jongh and A. R. Miedema, *Adv. Phys.* **23**, 1 (1974).
- ²⁴S. Tang and J. E. Hirsch, *Phys. Rev. B* **39**, 4548 (1989), and references therein.
- ²⁵See, e.g., C. J. Ballhausen, *Introduction to Ligand Field Theory* (McGraw-Hill, New York, 1962).
- ²⁶D. Shaltiel, H. Bill, P. Fischer, M. Francois, H. Hagemann, M. Peter, Y. Ravisekhar, W. Sadowski, H. J. Scheel, G. Triscone, E. Walker, and K. Yvon, *Physica C* **158**, 424 (1989).
- ²⁷M. Takigawa, P. C. Hammel, R. H. Heffner, and Z. Fisk, *Phys. Rev. B* **39**, 7371 (1989); M. Takigawa, P. C. Hammel, R. H. Heffner, Z. Fisk, J. L. Smith, and R. B. Schwarz, *ibid.* **39**, 300 (1989); C. H. Pennington, D. J. Durand, C. P. Slichter, J. P. Rice, E. D. Burkowski, and D. M. Ginsberg, *ibid.* **39**, 2902 (1989); F. Mila and T. M. Rice, *Physica C* **157**, 561 (1989).
- ²⁸P. W. Selwood, *Magnetochemistry* (Interscience, New York, 1956), p. 78.
- ²⁹T. C. Leung, X. W. Wang, and B. N. Harmon, *Phys. Rev. B* **37**, 384 (1988).
- ³⁰Y. J. Uemura, W. J. Kossler, J. R. Kempton, X. H. Yu, H. E. Schone, D. Opie, C. E. Stronach, J. H. Brewer, R. F. Kiefl, S. R. Kreitzman, G. M. Luke, T. Riseman, D. L. Williams, E. J. Ansaldo, Y. Endoh, E. Kudo, K. Yamada, D. C. Johnston, M. Alvarez, D. P. Goshorn, Y. Hidaka, M. Oda, Y. Enomoto, M. Suzuki, and T. Murakami, *Physica C* **153-155**, 769 (1988).
- ³¹K. Yamada, E. Kudo, Y. Endoh, Y. Hidaka, M. Oda, M. Suzuki, and T. Murakami, *Solid State Commun.* **64**, 753 (1987).